International Journal of Engineering Sciences & Research Technology

(A Peer Reviewed Online Journal)
Impact Factor: 5.164

IJESRT

RESEARCHERID
THOMSON REUTERS

[Mustafa *et al.*, 10(8): August, 2021]
IC™ Value: 3.00

ISSN: 2277-9655
Impact Factor: 5.164
CODEN: IJESS7

IJESRT

INTERNATIONAL JOURNAL OF ENGINEERING SCIENCES & RESEARCH TECHNOLOGY

APPLICATION OF ADRC AND PID CONTROLLER TO DISTRIBUTED LFC FOR AN INTERCONNECTED MULTI-AREA POWER SYSTEM

Mustafa Eltigani I. M.[*1], Uma Nangia[1] & Gomaa Haroun A. H.[2]

[1]Department of Electrical Engineering, Delhi Technological University, New Delhi, India
[2]Department of Electrical and Electronics Engineering, Faculty of Engineering, University of Nyala, Sudan

DOI: https://doi.org/10.29121/ijesrt.v10.i8.2021.3

ABSTRACT

This article addresses the application of active disturbance rejection control (ADRC) and classical PID controller to distributed load frequency control (LFC) for an interconnected multi-area power system. The proposed approach has been designed to improve the power system performances as well as to reduce the damping oscillations of the uncertainties due to variation in system parameters and load perturbations. Dynamic performances of an interconnected multi-areas power system are presented, and the effect of the generation rate constraint (GRC) is considered. The model was employed in the ADRC+PID architectures. Digital simulations for a 4-area power system are presented to validate the effectiveness of the proposed approach. The supremacy of the proposed controller is proved by comparing the results with that of the recently published paper based on the linear quadratic regulator (LQR) for the same system. The simulation results are compared among the proposed controller, ADRC technique alone, and conventional PID controller. Simulation results asserted that the proposed technique outperforms the other controllers in terms of fast settling time, and less in peak overshoot. The proposed ADRC+PID approach satisfies the LFC requirements with a reasonable dynamic response.

KEYWORDS: LFC, Interconnected multi-area power system, ADRC, Classical PID controller.

1. INTRODUCTION

The modern electrical power system consists of different power system units, such as hydro, thermal, and nuclear, and gas, these units are interconnected coherently through each other by transmissions lines (tie-lines) [1]. The main functions of an interconnected multi-area power system are: generating, transmitting, and distributing electrical power as economically and consistently as possible while maintaining the quality of the output power, and frequency within the acceptable limits [2]. Each control area has its generation unit which is responsible for its load perturbations and power interchange between the neighboring areas [1, 2]. In an interconnected area power system, if the load deviation occurred at any area of the system, the frequency associated with this area is affected firstly and the other areas are also affected according to this perturbation through transmission lines. With the enlargement of the power system size and increasing of the energy consumption in a recent year, the power systems became complex to satisfy the power needs of consumers.

The interconnected areas of power systems are confronting several challenges in terms of power system design, operation, and control [3, 4]. Since the load demand is varied arbitrarily in a power system, both frequencies of an interconnected area and the tie-line power are varied. It is impossible to maintain the balance between generation and load demand without control. Therefore, the control strategy is needed to reduce the effects of the random load changes and maintaining the frequency at the nominal value. The deviations in frequency and power interchange should be controlled by area control error (ACE). ACE can be defined as a linear combination of the frequency deviations in control areas and the active power flow interchange (tie-lines power) that connected with the neighbor areas. To handle the LFC problem, there are two frequency control loops, primary and supplementary control loops. LFC in power systems is the most significant in order to provide or supply reliable active power with a good quality [5]. Consequently, the tasks of LFC in interconnected multi-areas are to provide

ISSN: 2277-9655
Impact Factor: 5.164
CODEN: IJESS7

the desired real power output from the generator to meet the change in load, maintain the frequency of the power system close to the nominal value and maintain the scheduled interchange of power between control areas through tie-lines [6, 7]. Thus, the control scheme is required, that not only preserves constancy of frequency and desired output power but also attain zero steady-state error and inadvertently scheduled interchange.

Nowadays, the designers of the control system are trying to design and applying different control algorithms in order to find the best controller parameters to access the optimum solutions. Classical controllers like proportional-integral (PI) controller and proportional-integral-derivative (PID) controller are extensively applied in the power system to tackle or to solve the LFC issues [8-10]. However, the classical controllers are easy to tune and simple in architecture, but usually give a long settling time and produce large overshoot in the system responses [11]. Furthermore, the classical controllers are not robust against the disturbances and system uncertainties, consequently, classical controllers have many limitations as mentioned above, and may not be longer appropriate to work under all operating conditions. Therefore, sophisticated controllers have been established to improve the transient performances of LFC, despite the existence of load perturbations and parameters variations. Literature survey shows that there are several advanced controllers such as conventional, genetic algorithms (GAs), particle swarm optimization (PSO), fuzzy logic controller (FLC), artificial neural network, etc. have been applied for LFC to explore an optimum controller in addition to overcome the limitations of classical approaches [12-20]. GAs techniques have been extensively addressed for the design of load frequency control. The authors in Ref. [12], optimized the parameters of the PID sliding mode control of two area power systems via GAs considering the effects of nonlinearities. The optimal parameters of PID and fractional-order PID controllers have been optimized by GAs for a two-area electrical power system [13, 14]. Tuning of the decentralized controllers for a realistic system including physical constraints is considered in [15]. The authors in Ref. [16], optimized the parameters of the PI controllers by PSO using a new cost function. FLC is employed on a two-area interconnected power system according to [17], with reheat and hydro plants. But, the author not discussed the system robustness against parameter variations. Another Fuzzy PID controller is designed on two interconnected power system areas according to [18], with a reheat turbine and the author tested the controller under different load changes, but not takes into account the robustness of the controller approach against system uncertainties. In [19], a neural-fuzzy controller is applied for a two-area power system without adding the effect of the nonlinearities. An Intelligent technique based on the fuzzy logic controller is applied for a three interconnected multi areas power system in [20], with a reheat turbine, however, the nonlinearity effect is not considered in the system. In most articles of LFC, the researchers have been neglected the effects of the physical constraints for simplicity, But for the realistic analysis of system performances, it shall be adequate to include these effects.

Recently, some articles have been reported the application of the ADRC technique on the load frequency control issue [21-24]. In Ref. [21], the authors utilized the ADRC technique for a two-area power system, with non-reheat turbines, but, not discussed the system robustness against parameter variations and load changes. In Refs. [22, 23], fast dynamic responses, robustness against parameter variations, and load perturbations can be obtained using the ADRC controller, but the authors not considered the impacts of the physical constraints in the system model. In [24], a new technique of LFC is proposed for a two-area power system considering doubly-fed induction generator system-based wind turbine power systems using a linear ADRC technique.

This article sheds the light on the effects of parametric uncertainties in addition to the load perturbations in an interconnected 4-areas power system with a decentralized ADRC + PID controller-based LFC. Appropriate physical constraints like GRC have been considered for four equal areas of the non-reheat thermal power system. The power system with the proposed ADRC + PID technique has been verified over the effect of uncertainties due to parameters variations of the governor, turbine, synchronizing coefficient, and load perturbations. The superiority of the suggested ADRC + PID technique is validated by comparing the simulation results with a lately published article based on the linear quadratic regulator (LQR) for the same power system [25], and the model was implemented via MATLAB/SIMULINK. ADRC technique is considered an emerging technique, which estimates and mitigates uncertainties, and the results do not require accurate model information comparing with the other sophisticated controllers [23]. The ADRC approach has only two tuning parameters, and the structure is simple to implement in practice. In this paper, the ADRC is modified and employed in the power system with four thermal turbine units. The obtained results verified that the proposed technique outperforms the other controllers

ISSN: 2277-9655
Impact Factor: 5.164
CODEN: IJESS7

and guarantee robust performances in the presence of uncertainties caused by parameters variations in addition to the load perturbations.

The reset sections of the article are organized as follows: The mathematical modeling of an interconnected multi-area power system is presented in section 2. Section 3 gives an overview and structure design of the proposed controller. Simulation results and discussion is presented in section 4. Finally, the conclusion of the article is presented in section 5.

Nomenclature:

parameter	Description	Unit
$\Delta f_i(t)$	Frequency deviation of area i	Hz
$\Delta P_{mi}(t)$	Mechanical power deviation of area i	p.u.MW
$\Delta P_{tie,i}(t)$	Tie-line active power deviation of area i	p.u.MW
$\Delta P_{Li}(t)$	Load disturbance of area i	p.u.MW
M_i	Equivalent inertia constant of area i	p.u.s
D_i	Equivalent damping coefficient of area i	p.u/Hz
T_{ti}	The non-reheat turbine time constant of area i	s
T_{gi}	Thermal governor time constant of area i	s
B_i	Frequency bias factor of area i	p.u.MW/Hz
R_i	Speed drop due to governor action of area i	Hz/p.u.MW
T_{ij}	Synchronizing coefficient of area i	p.u.MW
ACE_i	Area control error of area i	p.u.MW

2. SYSTEMS INVESTIGATED

In this section, the general dynamic model of an interconnected four-area power system is demonstrated. A 4-area of an interconnected power system as depicted in Fig. 1, is used to explain the motivation of the suggested approach, as shown it consists of four non-reheat thermal plants. As demonstrated in Fig. 2, each area of the power plant consists of a single generator, single governor, and single turbine unit. The power generating unit consists of a generator, system governor, and turbine. Furthermore, as depicted in Fig. 2 each area includes three inputs, which are namely, the controller input $U(s)$, load disturbance $\Delta P_L(s)$, and tie-line power error $\Delta P_{tie}(s)$, besides the two outputs, which are area control error $Y(s)$ and generator output Δf. Fig. 2, ΔP_v represents the valve of gate position change, ΔP_e electrical power, and ΔP_m mechanical power. The area control error (ACE) is measured by the system output and can be defined by Eq. (1), for each area, where B denotes the area frequency bias setting [1].

$$ACE(t) = \Delta P_{tie}(t) + \mathrm{B}\,\Delta f(t) \tag{1}$$

In this article, we utilize the transfer function (TF) to model the generator unit for the sake of suitability in frequency-domain analyses. Let us consider the TF from $\Delta P_e(s)$ to $\Delta P_m(s)$ be $G_{ET}(s) = Num_{ET}(s)/Den_{ET}(s)$, where $Num_{ET}(s)$, and $Den_{ET}(s)$ are the numerator and denominator polynomials, respectively. According to Ref. [1], the transfer function of the non-reheat turbine system $G_{ET}(s)$ is written as:

$$G_{ET}(s) = \frac{Num_{ET}(s)}{Den_{ET}(s)} = \frac{1}{(T_g s+1)(T_t s+1)} \tag{2}$$

ISSN: 2277-9655
Impact Factor: 5.164
CODEN: IJESS7

The TF of the generator is:

$$G_{Gen}(s) = \frac{1}{Den_M(s)} = \frac{1}{Ms + D} \tag{3}$$

The parameters in Eqs. (2) and (3) are demonstrated in Nomenclature. From Fig. 2, the output $Y(s)$ is written as:

$$Y(s) = \mathrm{G}_p(s)U(s) + \mathrm{G}_D(s)\Delta \mathrm{P}_L(s) + \mathrm{G}_{tie}(s)\Delta \mathrm{P}_{tie}(s) \tag{4}$$

where $\mathrm{G}_p(s)$, $\mathrm{G}_D(s)$, and $\mathrm{G}_{tie}(s)$ are the transfer functions between the three inputs ($U(s)$, $\Delta \mathrm{P}_L(s)$ and $\Delta \mathrm{P}_{tie}(s)$) and area control error output $\mathrm{Y}(s)$. The three TF in Eq. (4) are expressed as:

$$G_p(s) = \frac{RBNum_{ET}(s)}{RDen_{ET}(s)\,\mathrm{Den}_M(s) + Num_{ET}(s)} \tag{5}$$

$$G_D(s) = \frac{-RBDen_{ET}(s)}{RDen_{ET}(s)\,\mathrm{Den}_M(s) + Num_{ET}(s)} \tag{6}$$

$$G_{tie}(s) = \frac{Num_{ET}(s) + RDen_{ET}(s)\,\mathrm{Den}_M(s) - RBDen_{ET}(s)}{RDen_{ET}(s)\,\mathrm{Den}_M(s) + Num_{ET}(s)} \tag{7}$$

The proposed ADRC+PID-based control system is demonstrated in Fig. 3, for area 1, under a decentralized control strategy. The ADRC+PID technique is built in each area and acting as a local LFC. Four decentralized areas are interconnected to each other by tie lines. Non-reheat turbine units are considered in four equal areas orderly. The parameter values of the plant are obtained from [25], and listed in Appendix A. Substitute the parameter values into the $\mathrm{G}_p(s)$ between the controller input $U(s)$ and ACE output, we will have

$$G_{pi}(s) = \frac{1.02}{0.001s^3 + 0.0441s^2 + 0.4023s + 1.02} \tag{8}$$

where $G_{pi}(s)$ denotes the TF for a four area $(i = 1, 2, 3, and\ 4)$. The design procedures of the controller and parameter tuning are presented in the following section.

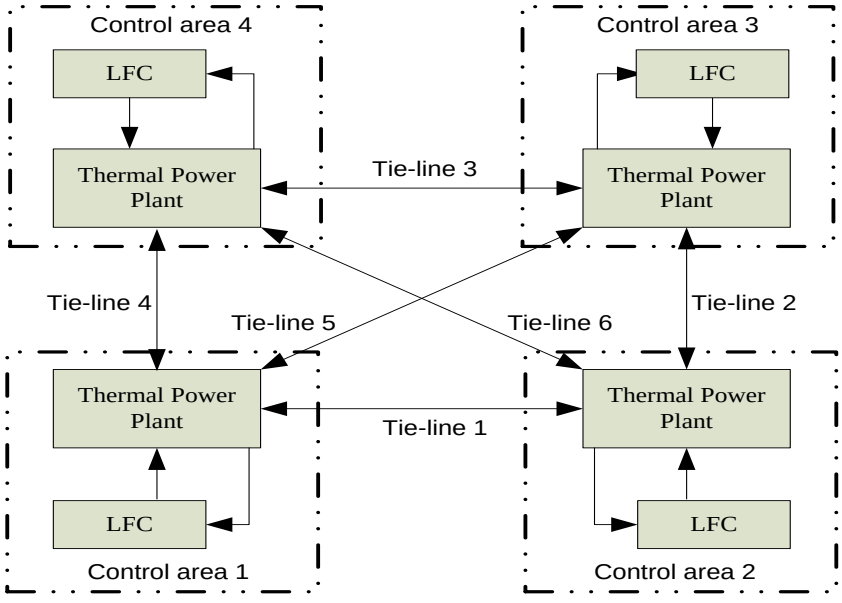

Fig. 1: Four interconnected control areas power system.

ISSN: 2277-9655
Impact Factor: 5.164
CODEN: IJESS7

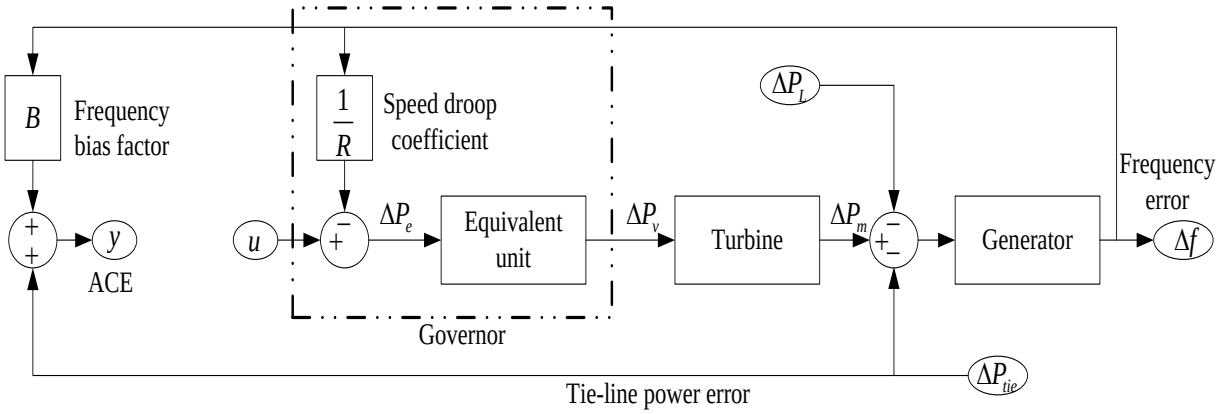

Fig. 2: Schematic diagram for the one-area generating unit.

3. THE DESIGN TECHNIQUES FOR LFC

We choose the ADRC+PID controller as a decentralized LFC for an interconnected four-area power system. The basic concept of the ADRC is introduced in [26]. In this article, the TF that characterized the ADRC will be established for a general n-th order plant.

3.1 Transfer function Derivation for n-th order system

Consider the system with a disturbance $W(s)$ as presented in Eq. (9):

$$Y(s) = G_P(s) \cdot U(s) + W(s) \tag{9}$$

where $\mathrm{U}(s)$ and $\mathrm{Y}(s)$ denotes the system input and system output respectively, and $W(s)$ the disturbance including the unknown internal dynamics and external disturbances. In general, the TF of the system $\mathrm{G}_p(s)$ can be written as

$$\frac{Y(s)}{U(s)} = G_p(\mathrm{s}) = \frac{b_m s^m + b_{m-1} s^{m-1} + \ldots + b_1 s + b_0}{a_n s^n + a_{n-1} s^{n-1} + \ldots + a_1 s + a_0}, \quad n \geq m \tag{10}$$

Where, a_i *and* $b_j (i = 1, \ldots, n, j = 1, \ldots, m)$ represents the polynomial coefficients of $\mathrm{G}_p(s)$. Divided both sides of the Eq. (9) by $\mathrm{G}_p(s)$, yield:

$$(1/G_p(s))Y(s) = U(s) + W^{'}(s) \tag{11}$$

where $W^{'}(s) = W(s)/Gp(s)$. In Eq. (11), the TF of $1/G_p(s)$ can be attained as

$$\frac{1}{\mathrm{G}_p(s)} = G_p(\mathrm{s}) = \frac{a_n s^n + a_{n-1} s^{n-1} + \ldots + a_1 s + a_0}{b_m s^m + b_{m-1} s^{m-1} + \ldots + b_1 s + b_0}, \quad n \geq m$$

$$= c_{n-m} s^{n-m} + c_{n-m-1} s^{n-m-1} + \ldots + c_1 s + c_0 + G_{rem}(s) \tag{12}$$

Where, $c_i (i = 0, \ldots, n-m)$ denotes the coefficients of $1/\mathrm{G}_p(s)$, and the remainder $G_{rem}(s)$ is:

$$G_{rem}(s) = \frac{d_{m-1} s^{m-1} + d_{m-2} s^{m-2} + \ldots + d_1 s + d_0}{b_m s^m + b_{m-1} s^{m-1} + \ldots + b_1 s + b_0} \tag{13}$$

where, d_j $(j = 0, \ldots, m-1)$ represents coefficients of the numerator of the $G_{rem}(s)$. Substitute Eq. (12) into Eq. (11), yield:

$$[c_{n-m} s^{n-m} + c_{n-m-1} s^{n-m-1} + \ldots + c_1 s + c_0 + G_{rem}(s)]\,\mathrm{Y(s)} = \mathrm{U(s)} + \mathrm{W}^{'}(\mathrm{s}) \tag{14}$$

ISSN: 2277-9655
Impact Factor: 5.164
CODEN: IJESS7

where $c_{n-m} = \frac{a_n}{b_m}$,

The Eq. (14), can be modeled in another form as:

$$c_{n-m}s^{n-m}Y(s) = U(s) - [c_{n-m-1}s^{n-m-1} + \ldots + c_1 s + c_0 + G_{rem}(s)]\mathrm{Y(s)} + W^{'}(s) \quad (15)$$

Dividing the Eq. (15) by c_{n-m} , yield:

$$s^{n-m}Y(s) = bU(s) + D(s) \quad (16)$$

Where $b = 1/c_{n-m}$ and

$$D(s) = -\frac{1}{c_{n-m}}[c_{n-m-1}s^{n-m-1} + \ldots + c_1 s + c_0 + G_{rem}(s)]\mathrm{Y(s)} + \frac{1}{c_{n-m}}W^{'}(s) \quad (17)$$

We use Eq. (16) as mentioned above to demonstrate the system model for the controller design.

3.2 Design of the extended state observer (ESO)

The robustness of the ADRC is depending on the precise estimation of the disturbance $D(s)$ [23, 26]. Therefore, the ESO needs to be developed in order to estimate the $D(s)$ in real-time. This can be carried out by augmenting the state variables of the system in Eq. (16) to include $D(s)$. Let $x_1(s) = Y(s)$. In order to demonstrate the ESO, the system modeled in Eq. (16), can be transformed as

$$sX(s) = AX(s) + BU(s) + E(s)D(s) \quad (18)$$

$$Y(s) = CX(s) \quad (19)$$

where

$$X(s) = \begin{bmatrix} x_1(s) \\ x_2(s) \\ . \\ . \\ . \\ x_{n-m}(s) \\ x_{n-m+1}(s) \end{bmatrix}, \quad A = \begin{bmatrix} 0 & 1 & 0 & . & . & . & 0 \\ 0 & 0 & 1 & . & . & . & 0 \\ . & . & . & . & & & . \\ . & . & . & & . & & . \\ . & . & . & & & . & . \\ 0 & 0 & 0 & . & . & . & 1 \\ 0 & 0 & 0 & . & . & . & 0 \end{bmatrix}_{(n-m+1)\times(n-m+1)}, \quad B = \begin{bmatrix} 0 \\ . \\ . \\ . \\ 0 \\ b \\ 0 \end{bmatrix}_{(n-m+1)\times 1}$$

$$E(s) = \begin{bmatrix} 0 \\ . \\ . \\ . \\ 0 \\ 0 \\ 1 \end{bmatrix}_{(n-m+1)\times 1}, \quad C = \begin{bmatrix} 1 & 0 & 0 & . & . & . & 0 \end{bmatrix}_{1\times(n-m+1)}$$

In order to derive the estimator, we suppose that $D(s)$ has the local Lipschitz continuity. Then the ESO is written as:

$$sZ(s) = AZ(s) + BU(s) + L(Y(s) - \hat{Y}(s)) \quad (20)$$

ISSN: 2277-9655
Impact Factor: 5.164
CODEN: IJESS7

$$\hat{Y}(s) = CZ(s) \tag{21}$$

where $Z(s)$ is the estimated state vector and $Z(s) = [z_1(s) \quad z_2(s) \quad . \quad . \quad . \quad z_{n-m}(s) \quad z_{n-m+1}(s)]^T$, and L is the observer gain vector and $L = [\beta_1 \quad \beta_2 \quad . \quad . \quad . \quad \beta_{n-m} \quad \beta_{n-m+1}]^T$. In order to set all the eigenvalues of the extended state observer to $(-\omega_0)$, the observer gains are selected as

$$\beta_i = \binom{n-m+1}{i} \cdot \omega_0^i, \qquad i = 1, 2, ..., n-m+1 \tag{22}$$

Therefore we can adjust and change the observer terms by setting or tuning the parameter ω_0, which denotes the bandwidth of the observer. With suitable tuned ESO, $z_i(s)$ can be able to approximate the value of $x_i(s)$ relatively $(i = 1, \ldots, n - m + 1)$, then we can write

$$z_{n-m+1}(s) = \hat{D}(s) \approx D(s) \tag{23}$$

where $\hat{D}(s)$ represents estimated $D(s)$.

3.3 Design of ADRC approach

The disturbance $D(s)$ can be removed, if the control input $U(s)$ is designed as:

$$U(s) = (U_0(s) - z_{n-m+1}(s))/b \tag{24}$$

The original system depicted in Eq. (16), will be reduced to a pure integral plant. This manner can be illustrated by Eq. (25), where $U_0(s)$ denote the control law for adjusting the ACE output $Y(s)$.

$$\begin{aligned} s^{n-m}Y(s) &= b \cdot [(U_0(s) - z_{n-m+1}(s))/b] + D(s) \\ &= U_0(s) - \hat{D}(s) + D(s) \approx U_0(s) \end{aligned} \tag{25}$$

The control aim of LFC is to regulate the ACE to zero. A classical PD controller can ensure this goal. So the control law $U_0(s)$ is selected as

$$U_0(s) = k_0(R(s) - z_1(s)) - k_1 z_2(s) - \cdots k_{n-m-1} z_{n-m-1}(s) \tag{26}$$

where $R(s)$ represent the reference input. In order to simplify the tuning procedure, all the closed-loop poles of the PD controller are set to $(-\omega_c)$. Then the controller gains in Eq. (26), have to be designed as

$$k_i = \binom{n-m}{i} \cdot \omega_c^{n-m-i}, \qquad i = 0, 1, ..., n-m-1 \tag{27}$$

where ω_c denote the bandwidth of the controller. If ω_c increasing the tracking speed of the output of the ADRC controlled system will increase. In other words, the tracking error, peak overshoot, and settling time of the output will decrease. Normally, ω_c varies from 3~10 rad/s. The general construction of the ADRC is given in Fig. 4.

ISSN: 2277-9655
Impact Factor: 5.164
CODEN: IJESS7

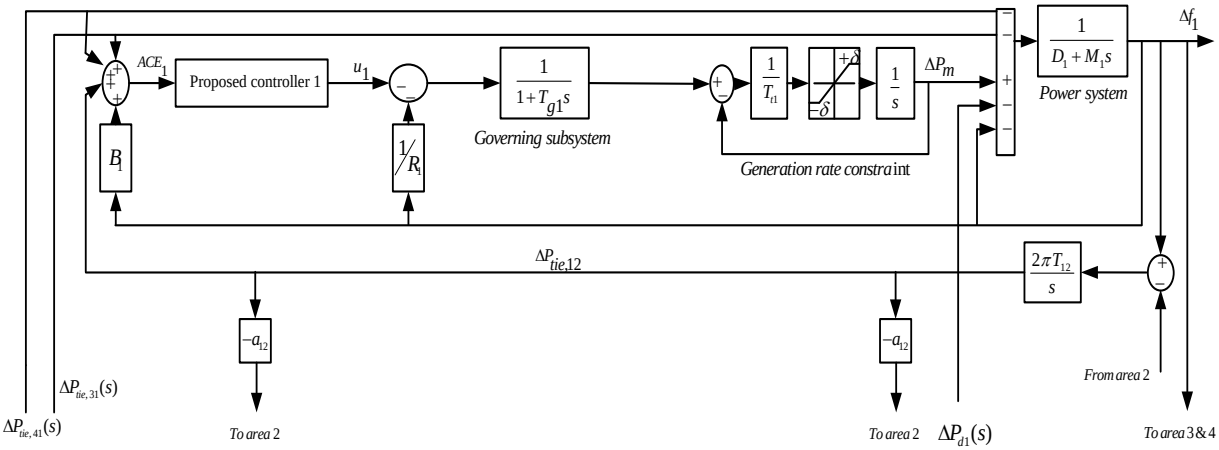

Fig. 3. Area 1 of four-area electrical power system

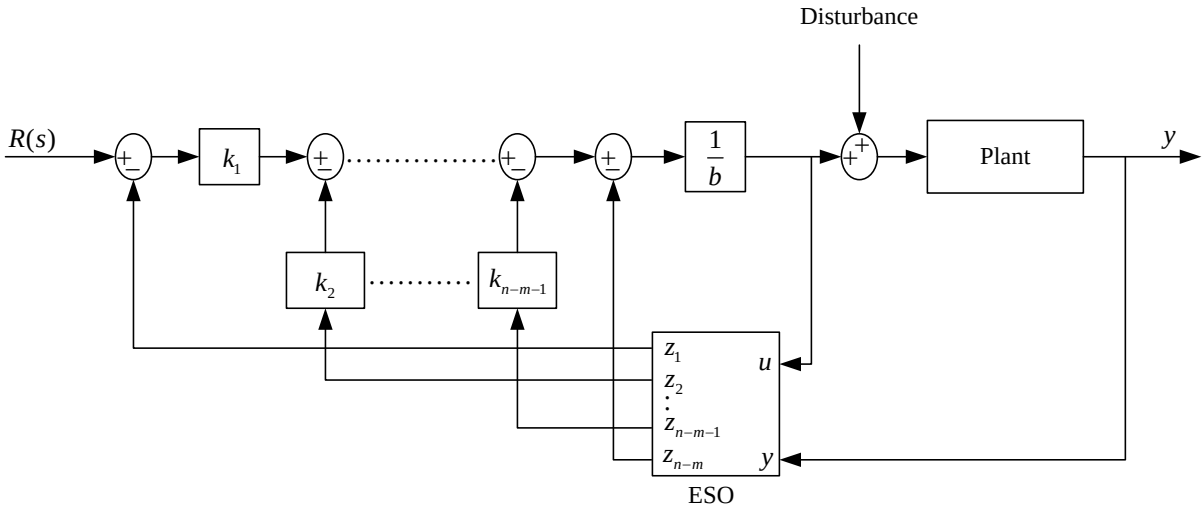

Fig. 4: General architecture for the ADRC approach

Table 1: ADRC parameters

	Order of ESO	ω_C	ω_O	b
Area 1	3	4	20	1020
Area 2	3	4	20	1020
Area 3	3	4	20	1020
Area 4	3	4	20	1020

4. SIMULATIONS RESULTS AND DISCUSSION

In order to validate or to check the effectiveness of the proposed ADRC+PID technique, some computer simulations have been carried out. The generation rate constraint (GRC) ($\delta = \pm 0.015$), [27-32], is considered for each area as depicted in Fig. 3. Parameters values of the power system are obtained from [25], and listed in Appendix A,

According to the detailed illustration in Section 3, the ADRC approach for area 1 of the power system can be designed and represented through the following equations.

$$sZ(s) = (A - LC)Z(s) + BU(s) + LY(s) \quad (28)$$

$$U_0(s) = k_0(R(s) - z_1(s)) - k_1 z_2(s) - k_2 z_3(s) \quad (29)$$

ISSN: 2277-9655
Impact Factor: 5.164
CODEN: IJESS7

$$U(s) = (\mathrm{U}_0(s) - z_4(s))/b \tag{30}$$

where,

$$Z(s) = \begin{bmatrix} z_1(s) \\ z_2(s) \\ z_3(s) \\ z_4(s) \end{bmatrix},\ A = \begin{bmatrix} 0 & 1 & 0 & 0 \\ 0 & 0 & 1 & 0 \\ 0 & 0 & 0 & 1 \\ 0 & 0 & 0 & 0 \end{bmatrix},\ B = \begin{bmatrix} 0 \\ 0 \\ b \\ 0 \end{bmatrix},\ L = \begin{bmatrix} 4\omega_0 \\ 6\omega_0^2 \\ 4\omega_0^3 \\ \omega_0^4 \end{bmatrix},\ C = [1 \quad 0 \quad 0 \quad 0],\ k_0 = \omega_c^3\ ,\ k_1 = 3\omega_c^2\ ,\ k_2 = 3\omega_c$$

The ADRCs for the other three areas have a similar architecture to area 1. The parameter values of the ADRCs approaches in four areas are presented in Table 1. There are only two tuning parameters for the design of ADRC, namely the controller bandwidth (ω_c) and the controller gain (b). For the PID controller, the gains of proportional, integral, and derivative are chosen as 0.5, -0.4, and 0.01 respectively, for all cases.

The performance of the proposed ADRC+PID controller is tested for three scenarios under the following operating conditions as follows:

4.1. Scenario 1

In this scenario, the simulation was performed by using the nominal system parameters as given in Appendix A, under applied load perturbation $\Delta P_{L1} = 0.01\, p.u.(\,per\,unit\,)$ to area 1. Fig. 5, depicts the simulation results of the proposed controller with the other controllers. Results from the upper to the bottom as shown in Fig. 5, are frequency deviations of the area 1-4, and the deviation in tie-line power $\Delta P_{tie,12}$. The frequency deviation of area 1 is presented in Fig. 6, on a large scale. The performance criteria index such as settling time and maximum overshoot of the frequency deviation, in addition to integral absolute error (IAE) as denoted in Eq. (31) are used to validate the dynamic performances of the proposed controller.

$$IAE = \int_0^\infty |\Delta f_i|\, dt \tag{31}$$

The frequency deviation of area 1 with settling time for 5% band of the step load perturbation, peak overshoots, and IAE are provided in Table 2. From simulation results of the frequency deviations and tie lines power, it verified that the proposed controller advocates its using for load frequency control (LFC), which is also confirmed via appropriate settlement of IAE. From the above comparison of the dynamic performances for controllers, it's cleared that the proposed controller provides better results in terms of fast settling time and less peak overshoot. Therefore, the out performances of the proposed controller appear to be more advantageous than the others controller and satisfying the demand for LFC.

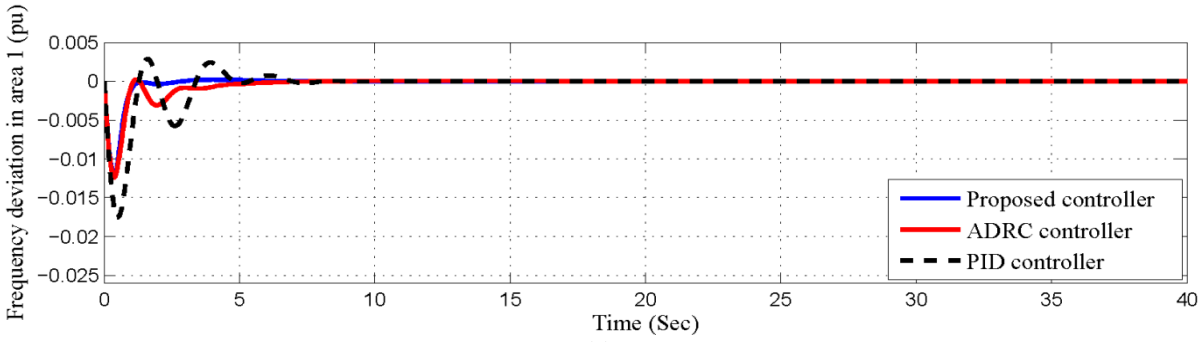

(a)

ISSN: 2277-9655
Impact Factor: 5.164
CODEN: IJESS7

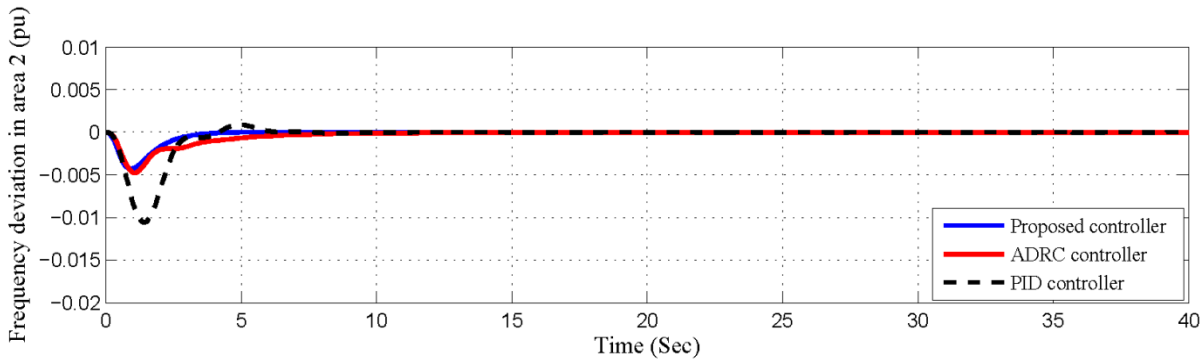

(b)

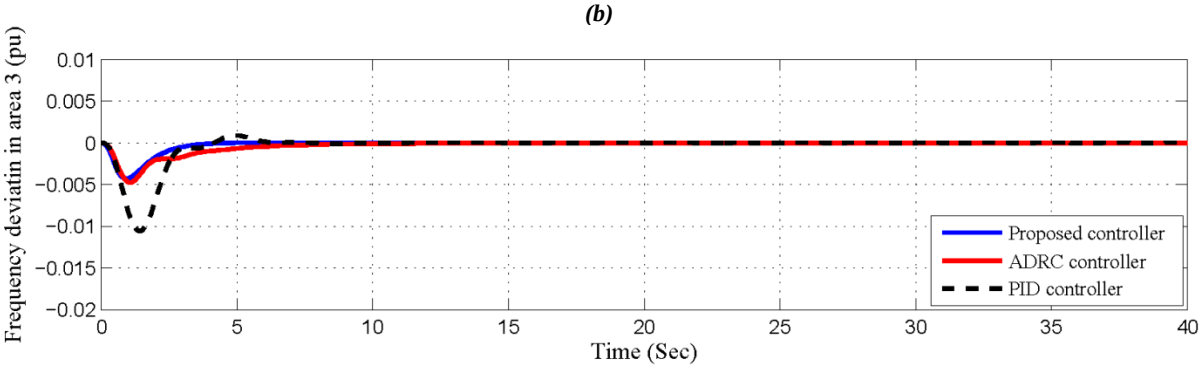

(c)

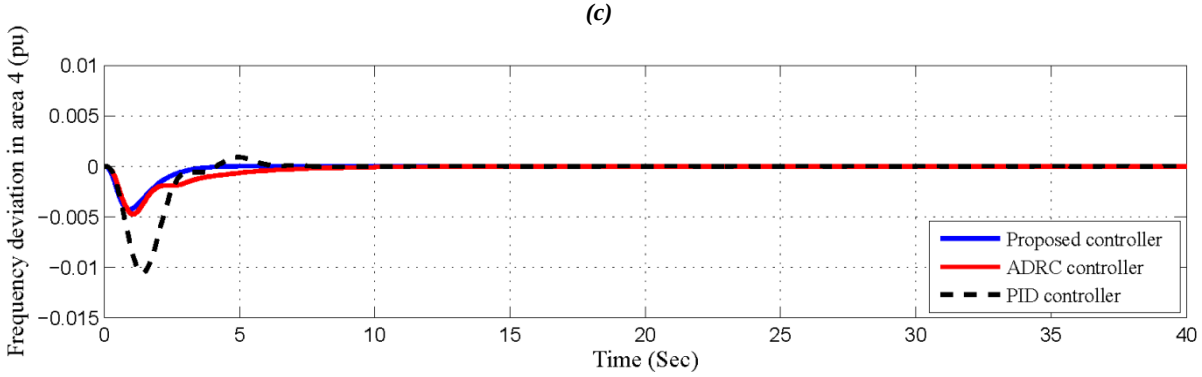

(d)

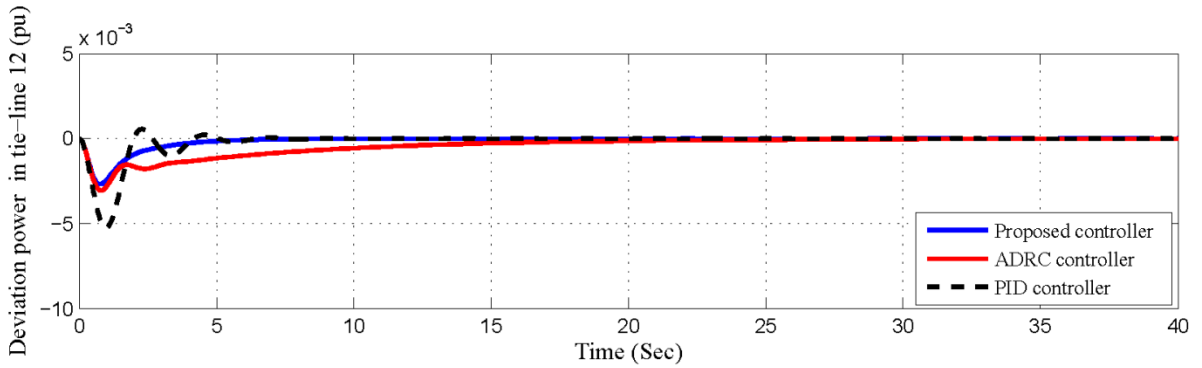

(e)

Fig. 5; System response for scenario 1: (a), (b), (c), and (d) represent frequency deviations in a four area and (e) the deviation in tie-line power $\Delta P_{tie,12}$ ***, in area 1.***

ISSN: 2277-9655
Impact Factor: 5.164
CODEN: IJESS7

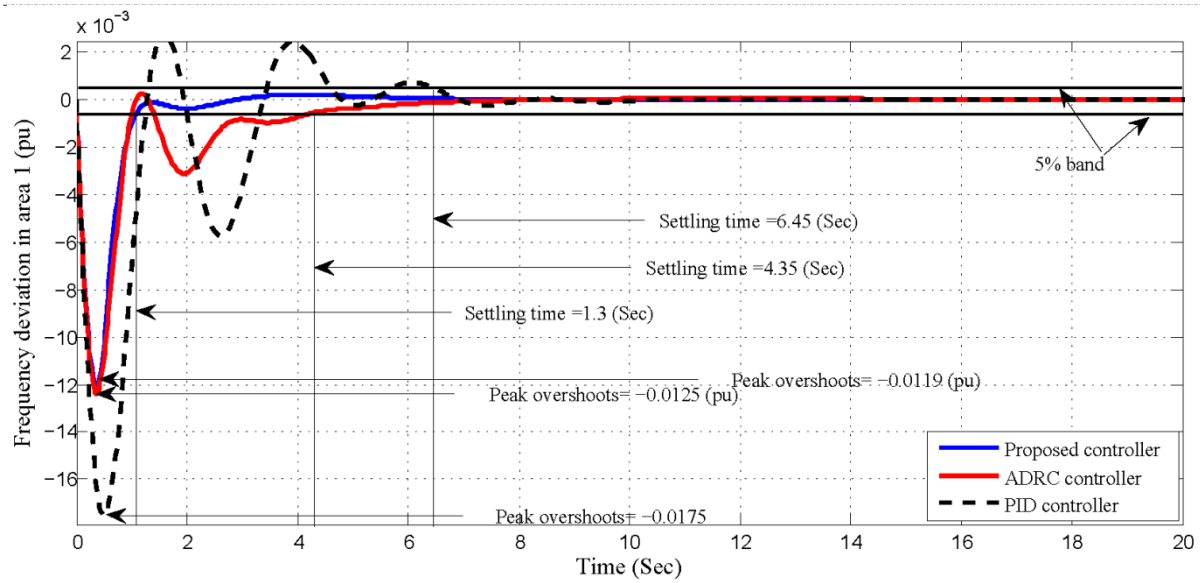

Fig. 6: The frequency deviations of area 1 in larger-scale indicating settling time for 0.01 change in load.

Table 2: Dynamic performance for Scenario 1

Controller	Settling time (sec) for 5% band	peak overshoot (Hz)	IAE
PID controller	6.4500	-0.0175	0.0229
ADRC controller	4.3500	-0.0125	0.0128
Ref. [25], for a four area system with (LQR)	1.8154	-0.0077	0.0046
Proposed controller	1.3000	-0.0119	0.0079

4.2. Scenario 2

Next, the robustness of the proposed controller against variations of the system parameters is assessed. This was done under an applied of 0.01p.u (per unit) load perturbation to area 1, while the system parameters are increased by +35%from the nominal value, mainly $\left(T_{gi},\ T_{ti}\ and\ T_{ij}\right)$. The frequency deviations for areas 1-4 and the tie-line power $\Delta P_{tie,12}$, are depicted in Fig. 6, respectively. The simulation results are given in Table 3. As clear from the Fig. 7, and Table 3; the robustness of the proposed approach against parameters variation is superior to the other controllers.

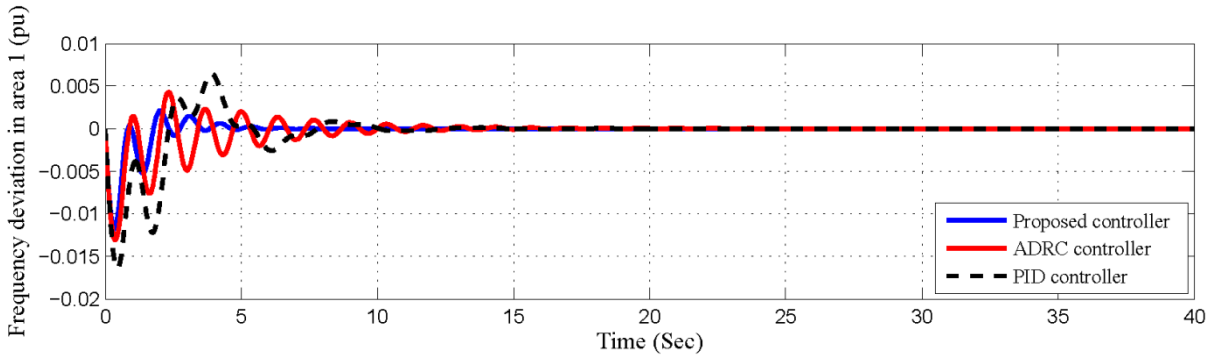

(a)

ISSN: 2277-9655
Impact Factor: 5.164
CODEN: IJESS7

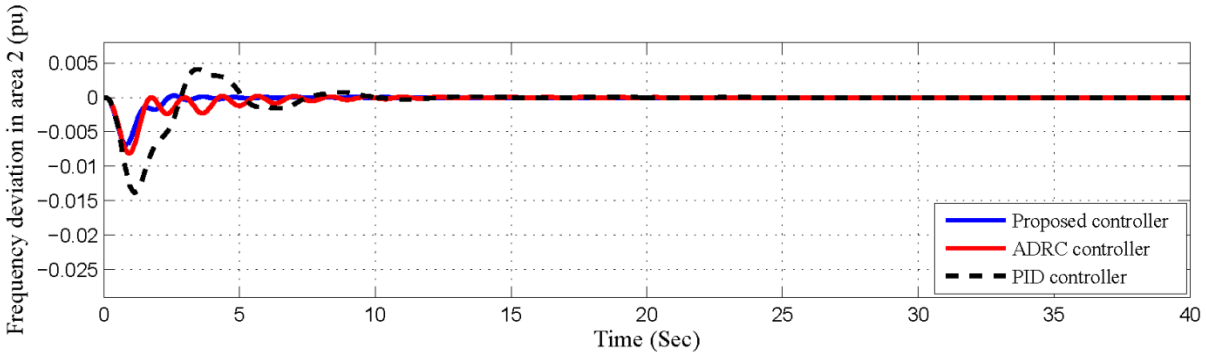

(b)

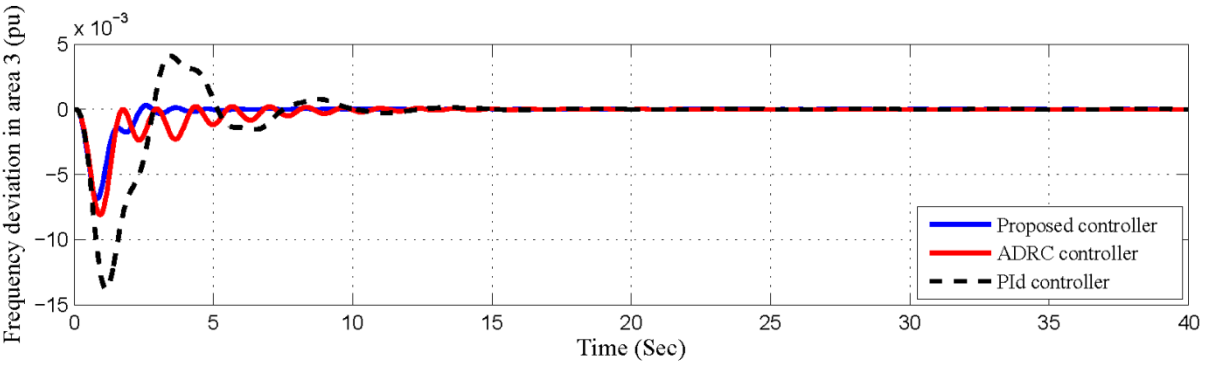

(c)

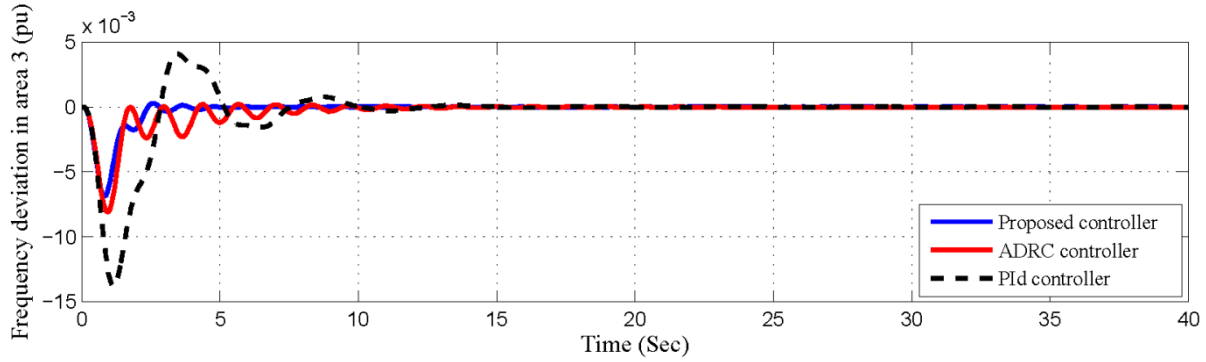

(d)

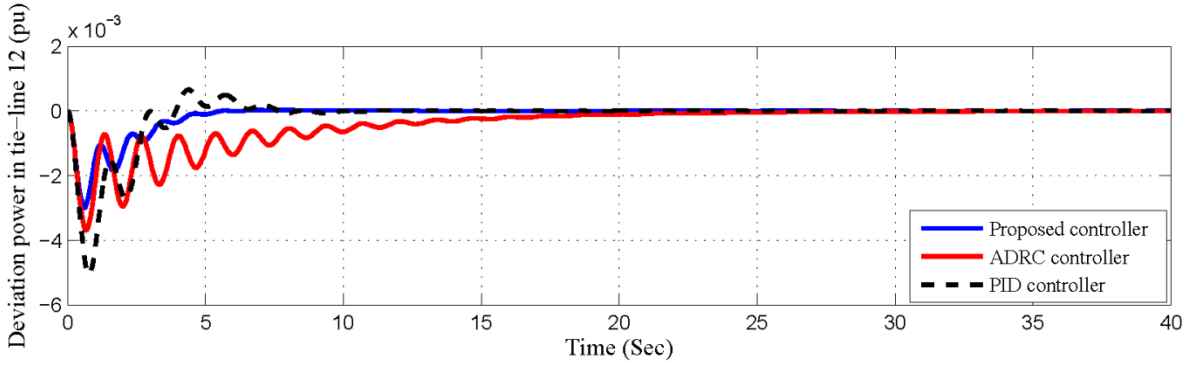

(e)

Fig. 7; System response for scenario 2: (a), (b), (c) and (d) represent frequency deviations in a four area and (e) the deviation in tie line power $\Delta P_{tie,12}$, in area 1.

ISSN: 2277-9655
Impact Factor: 5.164
CODEN: IJESS7

Table 3: Dynamic performance for Scenario 2

Controller	Settling time (sec) for 5% band	peak overshoot (Hz)	IAE
PID controller	8.7540	-0.0164	0.0338
ADRC controller	10.3300	-0.0129	0.0230
Proposed controller	4.3960	-0.0114	0.0104

4.3. Scenario 3

Finally, to supported the efficiency of the suggested controller, system has been verified in another case, in this case the system parameters of each area have been decreasing by -35% , mainly $\left(T_{gi},\ T_{ti}\ and\ T_{ij} \right)$ under applied 0.01p.u as step load perturbation in area 1, as same as for the other two scenarios. The Dynamic performances are depicted in Fig. 8, and Table 4. Again, the supremacy of the proposed controller is proved, in spite of the extremely variations in system parameters and load disturbances.

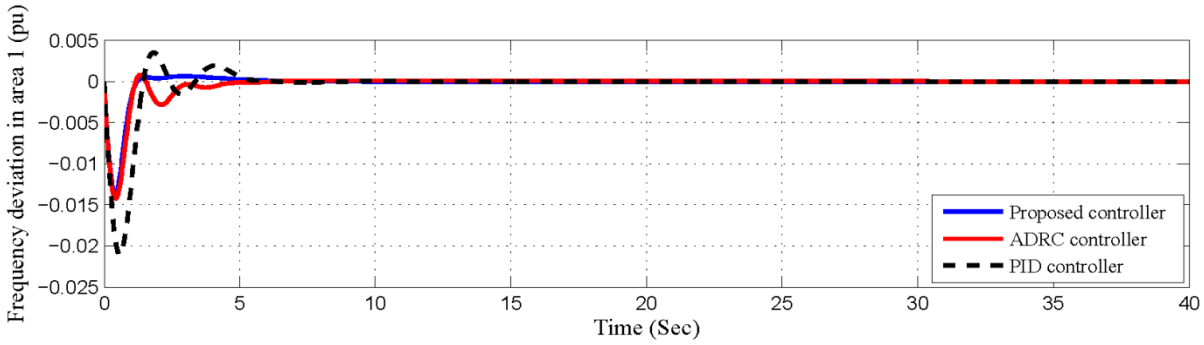

(a)

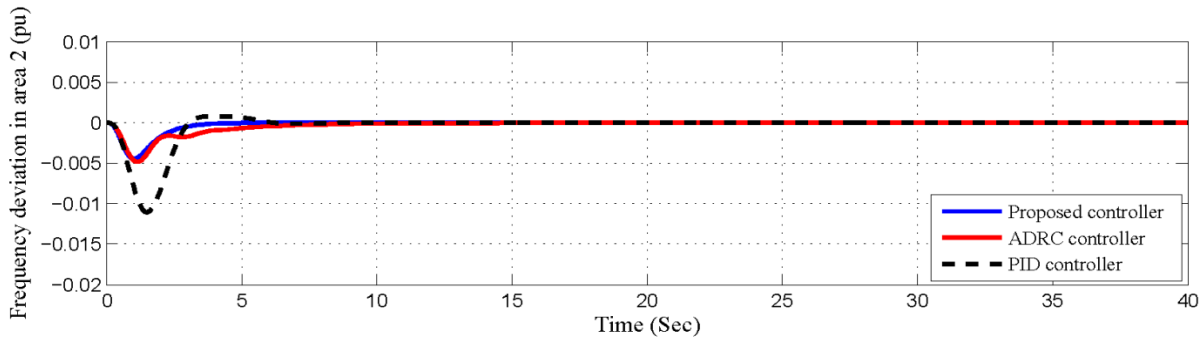

(b)

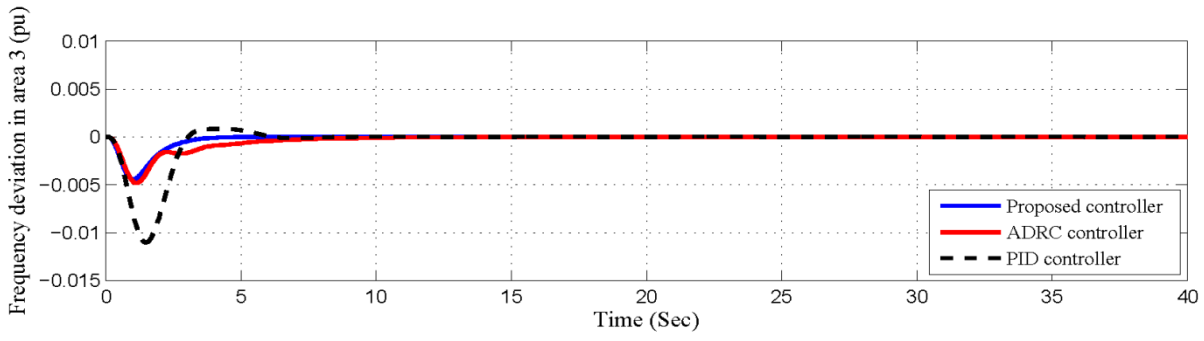

(c)

ISSN: 2277-9655
Impact Factor: 5.164
CODEN: IJESS7

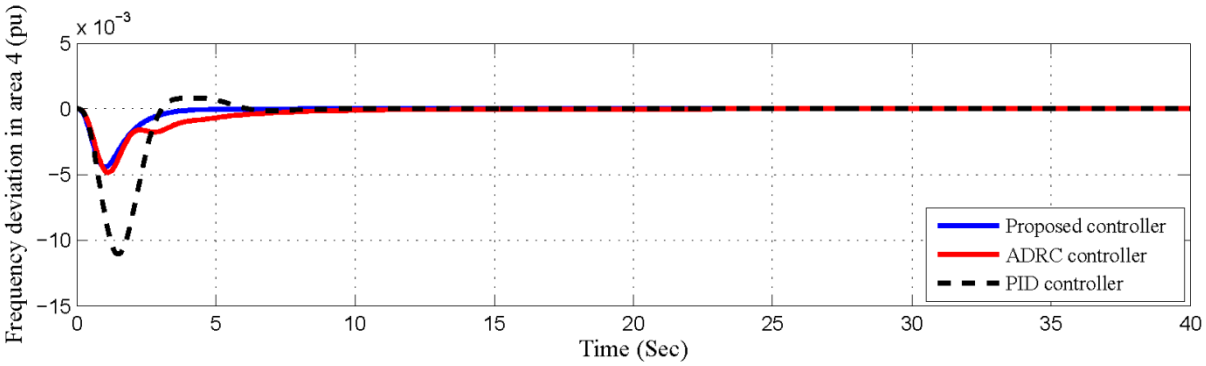

(d)

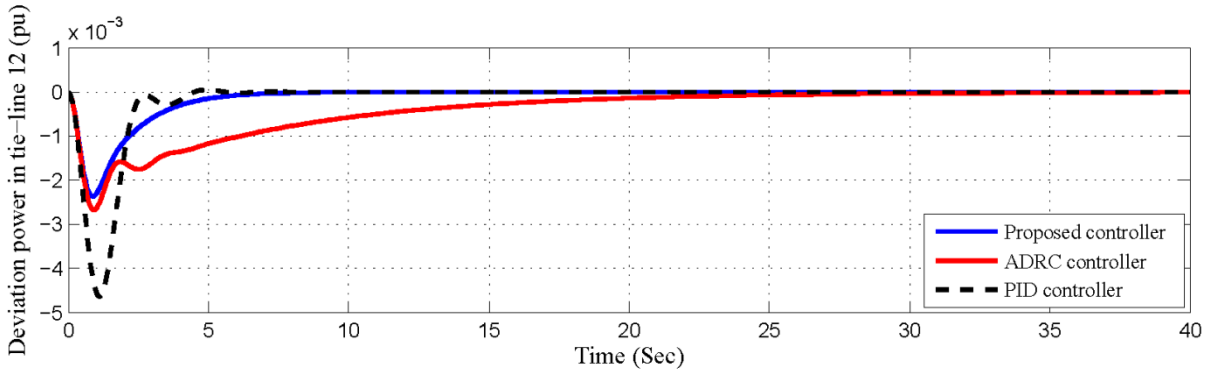

(e)

Fig. 8; System response for scenario 3: (a), (b) , (c) and (d) represent frequency deviations in a four area and (e) the deviation in tie line power $\Delta P_{tie,12}$, in area 1.

Table 4: Dynamic performance for Scenario 3

Controller	Settling time (sec) for 5% band	peak overshoot (Hz)	IAE
PID controller	5.0580	-0.0210	0.0238
ADRC controller	4.2480	-0.0142	0.0145
Proposed controller	3.7860	-0.0120	0.0109

5. CONCLUSION

In this article, a new technique based on ADRC+PID controller is applied to a four non-reheat area power system in order to tackle the load frequency control problem. In this article, the classical PID controller and ADRC controller are combined and tuned in parallel. In order to prove the superiority of the proposed method, the simulation results are compared with that of a recently published article based on linear quadratic regulator (LQR) for LFC. From the simulations results we observed that the ADRC+PID controller gives superior dynamic performances. The performance analyses of the proposed controller have been compared with the ADRC technique alone, and PID controller. It proved that from the simulation results, the proposed controller exhibit better performance than the other controllers, in terms of settling time, peak overshoot, and the IAE. According to above simulation results in all scenarios, it is verified that the proposed controller makes the load frequency more robust and stable than the other controllers despite a wide variations in system's parameters.

Appendix A: System parameters:

Parameter		Unit
Rating	2000	MW
$P_{tie,\max}$	200	MW
M_i	0.1667	p.u.s
D_i	0.008333	p.u/Hz

ISSN: 2277-9655
Impact Factor: 5.164
CODEN: IJESS7

T_{ti}	0.03	s
T_{gi}	0.08	s
B_i	0.425	p.u.MW/Hz
R_i	2.4	Hz/p.u.MW
ΔP_{L1}	0.01	p.u.MW
a_{ij}	1.0	
T_{ij}	0.08674	p.u.MW

Notice: $i = 1, 2, 3 \; and \; 4$.

REFERENCES

[1] Kundur, P., N.J. Balu, and M.G. Lauby, Power system stability and control. Vol. 7. 1994: McGraw-hill New York.
[2] Arya, Y., N. Kumar, and S. Sinha, Fuzzy logic based load frequency control of multi-area electrical power system considering non-linearities and boiler dynamics. International Energy Journal, 2012. 13(2): p. 97-111.
[3] GUO, J. and L. DONG, Sliding Mode Based Load Frequency Control for a Two-area Interconnected Power System. International Journal of Intelligent Control and Systems, 2015. 20(1): p. 16-25.
[4] Kumar, N.V. and M.M.T. Ansari, A new design of dual-mode Type-II fuzzy logic load frequency controller for interconnected power systems with parallel AC–DC tie-lines and superconducting magnetic energy storage unit. Energy, 2015. 89: p. 118-137.
[5] Çam, E. and I. Kocaarslan, Load frequency control in two area power systems using fuzzy logic controller. Energy Conversion and Management, 2005. 46(2): p. 233-243.
[6] Zhang, Y., X. Liu, and Y. Yan, Model predictive control for load frequency control with wind turbines. Journal of Control Science and Engineering, 2015. 2015: p. 49.
[7] Sahu, R.K., S. Panda, and N.K. Yegireddy, A novel hybrid DEPS optimized fuzzy PI/PID controller for load frequency control of multi-area interconnected power systems. Journal of Process Control, 2014. 24(10): p. 1596-1608.
[8] Bevrani, H. and T. Hiyama, Robust decentralised PI based LFC design for time delay power systems. Energy Conversion and Management, 2008. 49(2): p. 193-204.
[9] Shayeghi, H., H. Shayanfar, and A. Jalili, Load frequency control strategies: A state-of-the-art survey for the researcher. Energy Conversion and management, 2009. 50(2): p. 344-353.
[10] Tan, W., Unified tuning of PID load frequency controller for power systems via IMC. IEEE Transactions on power systems, 2010. 25(1): p. 341-350.
[11] Panda, G., S. Panda, and C. Ardil, Automatic Generation Control of Interconnected Power System with Generation Rate Constraintsby Hybrid Neuro Fuzzy Approach. International Journal of Electrical and Electronics Engineering, 2009.
[12] Pingkang, L., Z. Hengjun, and L. Yuyun. Genetic algorithm optimization for AGC of multi-area power systems. in TENCON'02. Proceedings. 2002 IEEE Region 10 Conference on Computers, Communications, Control and Power Engineering. 2002. IEEE.
[13] Ghoshal, S., Application of GA/GA-SA based fuzzy automatic generation control of a multi-area thermal generating system. Electric Power Systems Research, 2004. 70(2): p. 115-127.
[14] Ismayil, C., R.S. Kumar, and T.K. Sindhu, Optimal fractional order PID controller for automatic generation control of two-area power systems. International Transactions on Electrical Energy Systems, 2015. 25(12): p. 3329-3348.
[15] Golpira, H. and H. Bevrani, Application of GA optimization for automatic generation control design in an interconnected power system. Energy Conversion and Management, 2011. 52(5): p. 2247-2255.
[16] Gozde, H., et al., Particle swarm optimization based pi-controller design to load-frequency control of a two area reheat thermal power system. ISI BILIMI VE TEKNIGI DERGISI-Journal OF Thermal Science AND Technology, 2010. 30(1): p. 13-21.
[17] Anand, B. and A.E. Jeyakumar, Fuzzy logic based load frequency control of hydrothermal system with non-linearities. International journal of electrical and power engineering, 2009. 3(2): p. 112-118.

ISSN: 2277-9655
Impact Factor: 5.164
CODEN: IJESS7

[18] RamaSudha, K., V. Vakula, and R.V. Shanthi, PSO based design of robust controller for two area load frequency control with nonlinearities. International Journal of Engineering Science and Technology, 2010. 2(5): p. 1311-1324.
[19] Francis, R. and I. Chidambaram, Control performance standard based load frequency control of a two area reheat interconnected power system considering governor dead band nonlinearity using fuzzy neural network. International Journal of Computer Applications, 2012. 46(15).
[20] Soundarrajan, A. and S. Sumathi, Effect of Non-linearities in fuzzy based load frequency control. International Journal of Electronic Engineering Research, 2009. 1(1): p. 37-51.
[21] Krishnarayalu, M. and K. Nagarjuna, ADRC for Two-Area LFC. International Journal of Engineering Research & Technology (UERT), 2014. 3(11): p. 141-146.
[22] Dong, L. and Y. Zhang. On design of a robust load frequency controller for interconnected power systems. in American Control Conference (ACC), 2010. 2010. IEEE.
[23] Dong, L., Y. Zhang, and Z. Gao, A robust decentralized load frequency controller for interconnected power systems. ISA transactions, 2012. 51(3): p. 410-419.
[24] Tang, Y., et al., Linear active disturbance rejection-based load frequency control concerning high penetration of wind energy. Energy Conversion and Management, 2015. 95: p. 259-271.
[25] Arya, Y., N. Kumar, and S. Gupta, Load frequency control of a four-area power system using linear quadratic regulator. International Journal of Energy Science, 2012. 2(2).
[26] Sun, B. and Z. Gao, A DSP-based active disturbance rejection control design for a 1-kW H-bridge DC-DC power converter. IEEE Transactions on Industrial Electronics, 2005. 52(5): p. 1271-1277.
[27] Arya, Y., H. Mathur, and S. Gupta, A novel approach for load frequency control of interconnected thermal power stations. International Journal of Energy Optimization and Engineering (IJEOE), 2012. 1(2): p. 85-95.
[28] Gomaa Haroun, A. H., and Yin-Ya Li. "A novel optimized hybrid fuzzy logic intelligent PID controller for an interconnected multi-area power system with physical constraints and boiler dynamics." ISA transactions 71 (2017): 364-379.
[29] Gomaa Haroun, A.H. and Yin-Ya, L., 2019. A novel optimized fractional-order hybrid fuzzy intelligent PID controller for interconnected realistic power systems. Transactions of the Institute of Measurement and Control, 41(11), pp.3065-3080.
[30] Gomaa Haroun, A. H., and Yin-Ya Li. "Ant lion optimized fractional order fuzzy pre-compensated intelligent pid controller for frequency stabilization of interconnected multi-area power systems." Applied System Innovation 2, no. 2 (2019): 17.
[31] Gomaa Haroun, A. H., and Yin-Ya Li. "On design of a robust decentralized controller for an interconnected multi-area power system with FACTS devices." FES Journal of Engineering Sciences 8, no. 2 (2019): 48-71.
[32] Gomaa Haroun, A. H., and Yin-Ya Li. "Ant lion optimized hybrid intelligent PID-based sliding mode controller for frequency regulation of interconnected multi-area power systems." Transactions of the Institute of Measurement and Control 42, no. 9 (2020): 1594-1617.